A bromine-rich artificial interphase to regulate interfacial kinetics in boron-centered electrolytes for magnesium metal batteries

Deviprasath Chinnadurai,†*[a] Gaoliang Yang,†*[a] Sonal Kumar,[a] Shengnan Sun,[a] Jianbiao Wang,[a] Zhenxiang Xing,[a] Debbie Hwee Leng Seng,[a] Zdenek Sofer[b] and Zhi Wei Seh*[a]

[a.] Institute of Materials Research and Engineering (IMRE), Agency for Science, Technology and Research (A*STAR), 2 Fusionopolis Way, Innovis #08-03, Singapore 138634, Republic of Singapore.

[b.] Department of Inorganic Chemistry, University of Chemistry and Technology, Prague, Technická 5, Prague 616628, Czech Republic.

E-mail: deviprasath_chinnadurai@a-star.edu.sg; yang_gaoliang@a-star.edu.sg; sehzw@a-star.edu.sg

† These authors contributed equally to this work.

Experimental

Material characterization

Structural and morphological characterizations were performed using a JEOL 6700F scanning electron microscope (SEM). The crystal structure of Mg foils was analyzed by X-ray diffraction (XRD, Bruker) with Cu Kα radiation (λ = 1.5418 Å). Elemental composition was examined using X-ray photoelectron spectroscopy (XPS, Thermo Fisher Scientific) with Al Kα radiation (1486.6 eV), and time-of-flight secondary ion mass spectrometry (TOF-SIMS, IONTOF GmbH, Germany).

Electrochemical measurements

All the electrochemical measurements were carried out in CR2032-type coin cells assembled in an argon-filled glovebox. Symmetric cells were fabricated using either bare Mg or Br-Mg anodes (⌀12.7 mm) as both counter and working electrodes, while asymmetric cells employed bare Mg or Br-Mg as the counter electrode and Al/C foil (⌀11.28 mm) as the working electrode. A glass fiber separator (Whatman™ GF/D), pre-dried in a vacuum oven at 150 °C for 4 h, was used in all cells. The electrolyte was prepared by dissolving 0.3 M magnesium tetrakis(hexafluoroisopropyloxy)borate ($Mg[B(hfip)_4]_2$, 99.99%, MTI) in 1,2-dimethoxyethane (DME, 99.5%, anhydrous, Sigma-Aldrich) pre-dried with molecular sieves (3 Å beads, 4–8 mesh, Sigma-Aldrich). Following preparation, the electrolyte was further dried over molecular sieves to ensure complete removal of residual moisture, and 80 µL was used per cell. The electrochemical performance of symmetric and asymmetric cells was evaluated using a Neware battery tester. Tafel and electrochemical impedance spectroscopy (EIS) measurements were performed in symmetric coin cells with a Gamry Reference 600+ Potentiostat, applying a 5 mV perturbation over a frequency range of 1 MHz to 0.01 Hz. For full-cell testing, Mo_6S_8 prepared following previously reported methods[1] was employed as the cathode material. The Mo_6S_8 cathode was fabricated by mixing Mo_6S_8 powder, Super P carbon, and polyvinylidene difluoride (PVDF) binder in a weight ratio of 8:1:1 to form a slurry, which was subsequently coated onto nickel foil. The electrodes were dried under vacuum at 60 °C overnight, yielding a mass loading of ~1.55 mg cm^{-2}, and tested at 0.1 C (1 C = 129 mA g^{-1}).

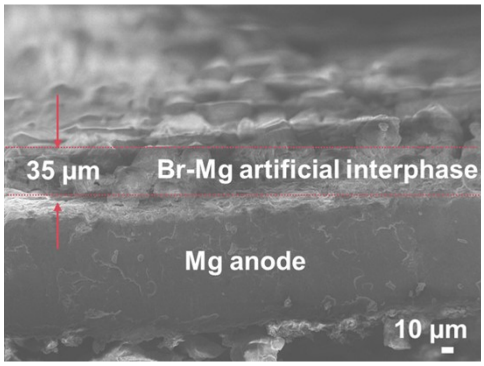

Figure S1. Cross sectional SEM image of Br-Mg anode.

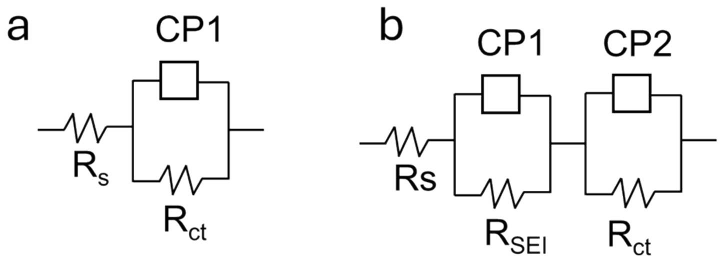

Figure S2. The equivalent circuit models employed to fit the Nyquist plots.

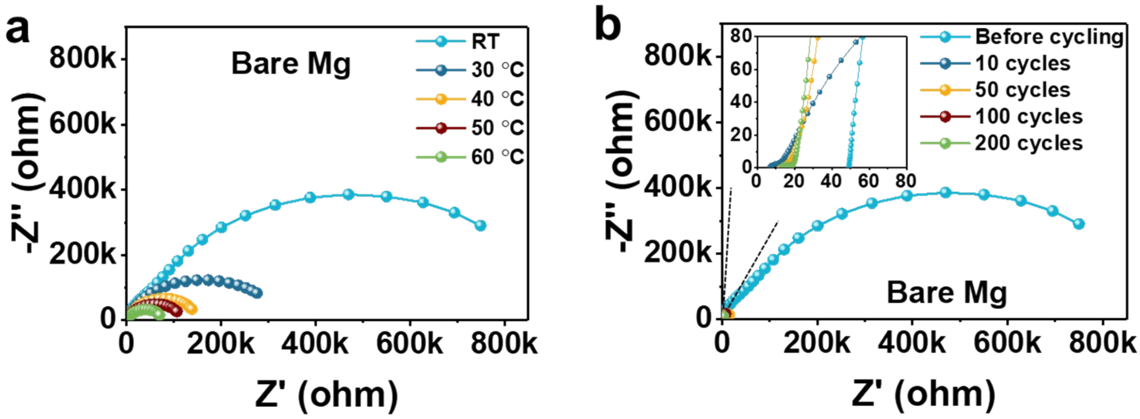

Figure S3. (a) Nyquist plots measured at different temperatures with bare Mg anode symmetric cell. (b) Nyquist plots measured at different cycles with bare Mg anode symmetric cell.

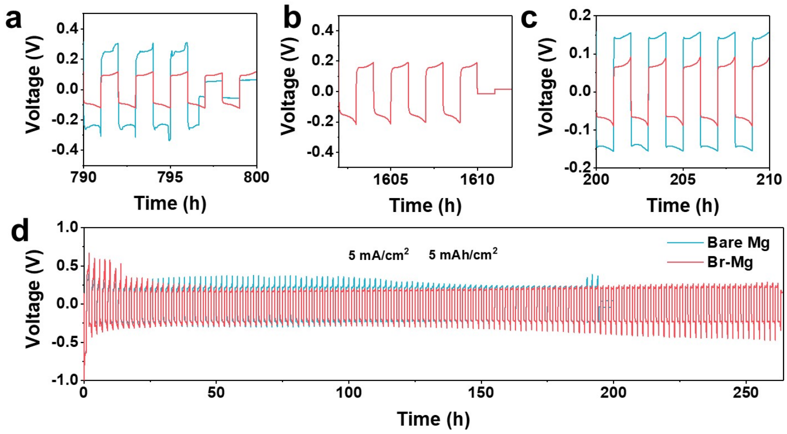

Figure S4. (a-c) Different time stamps of voltage profiles of symmetric cells measured at 0.5 mA cm^{-2} and 0.5 mAh cm^{-2}. (d) Galvanostatic cycling profiles of symmetric cells at 5 mA cm^{-2} and 5 mAh cm^{-2}.

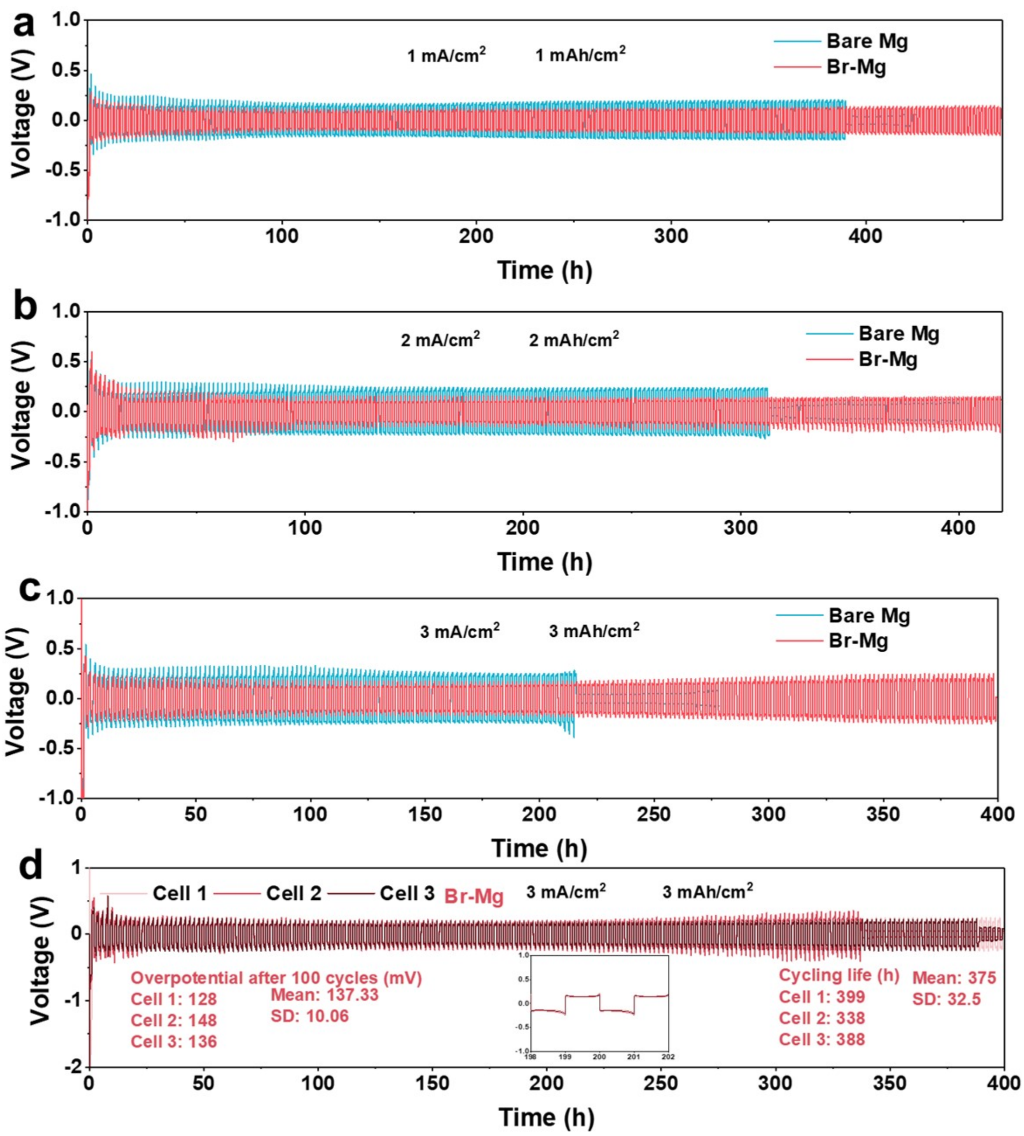

Figure S5. Galvanostatic cycling profiles of symmetric cells at (a) 1 mA cm^{-2} and 1 mAh cm^{-2}, (b) 2 mA cm^{-2} and 2 mAh cm^{-2}, (c) 3 mA cm^{-2} and 3 mAh cm^{-2}, (d) 3 mA cm^{-2} and 3 mAh cm^{-2} with three different cells with Br-Mg anode.

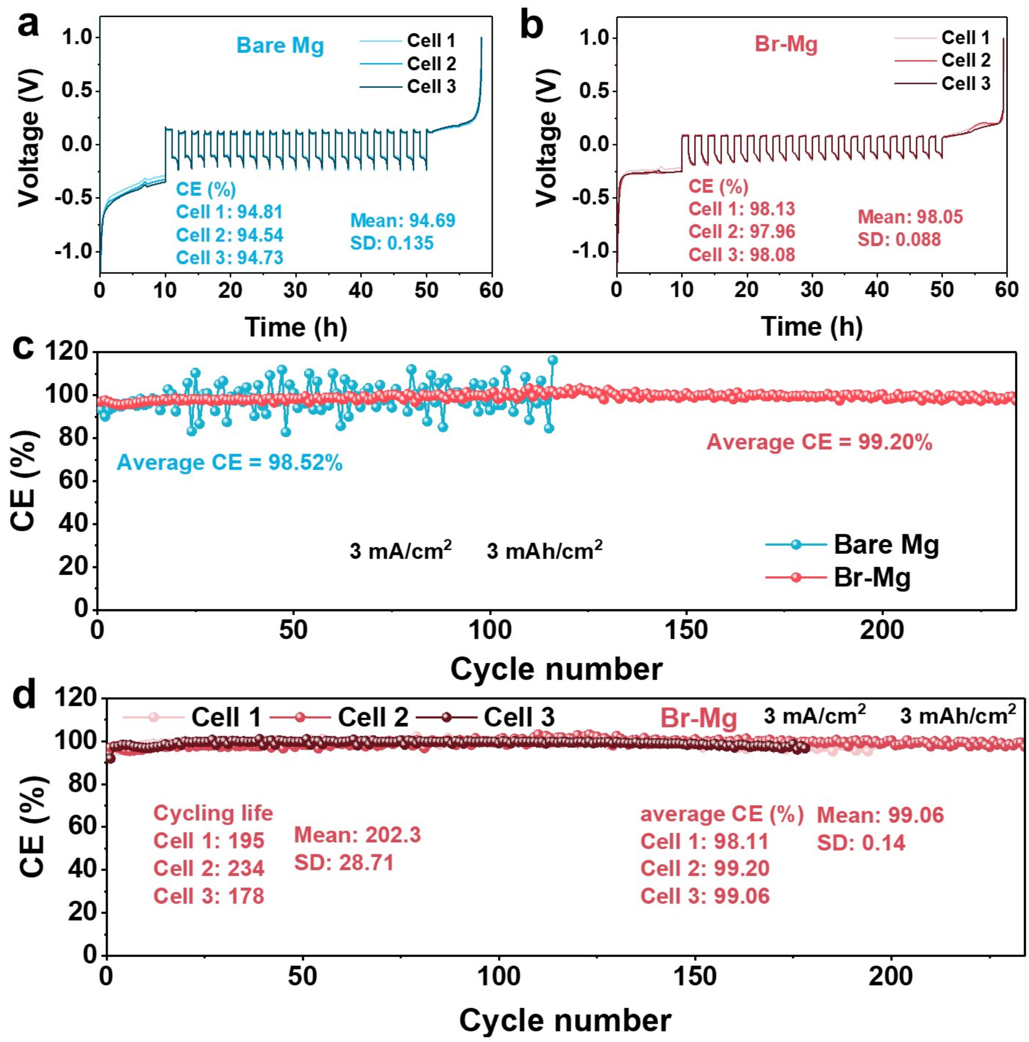

Figure S6. Galvanostatic profile of the asymmetric cells (a) Aurbach test of three different cells with bare Mg anode, (b) Aurbach test of three different cells with Br-Mg anode, (c) cells with different anodes at 3 mA cm^{-2} and 3 mAh cm^{-2}, (d) with three different cells with Br-Mg anode 3 mA cm^{-2} and 3 mAh cm^{-2}.

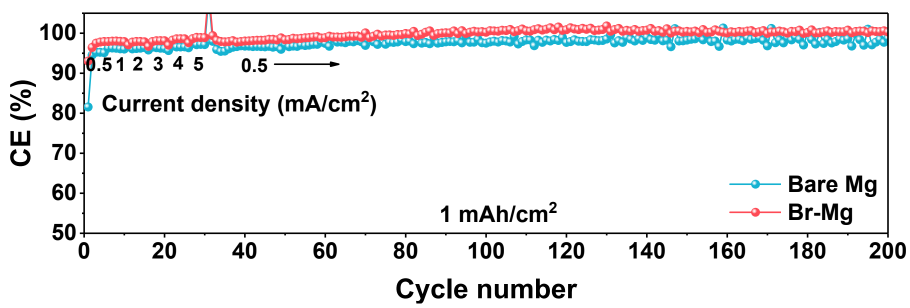

Figure S7. CE vs cycle number curves of asymmetric cells measured at different current densities.

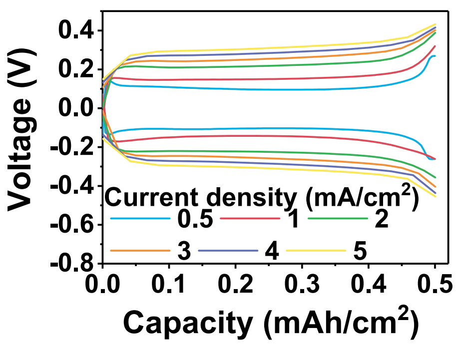

Figure S8. Voltage profile of the bare Mg symmetric cell measured at different current densities.

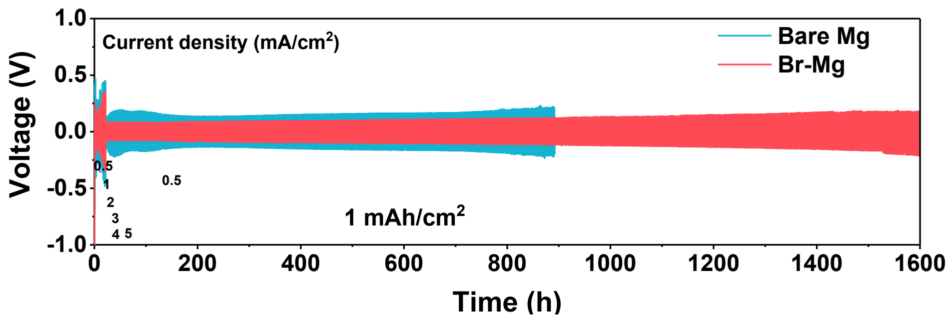

Figure S9. Galvanostatic cycling profile of the symmetric cells measured at different current densities.

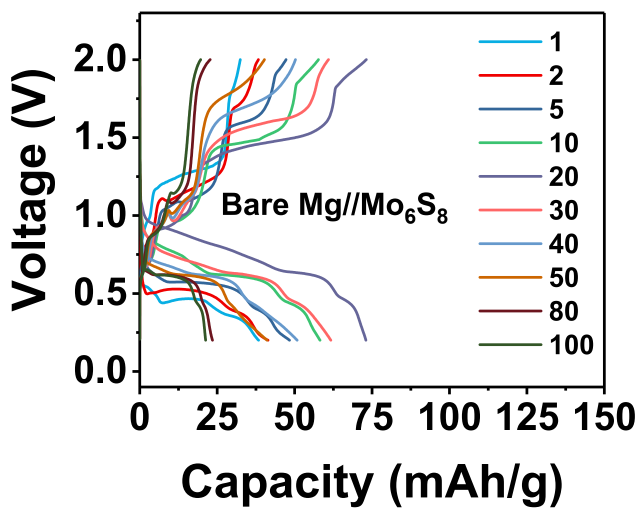

Figure S10. Voltage profile of the bare Mg//Mo_6S_8 full cell measured at 0.1 C.

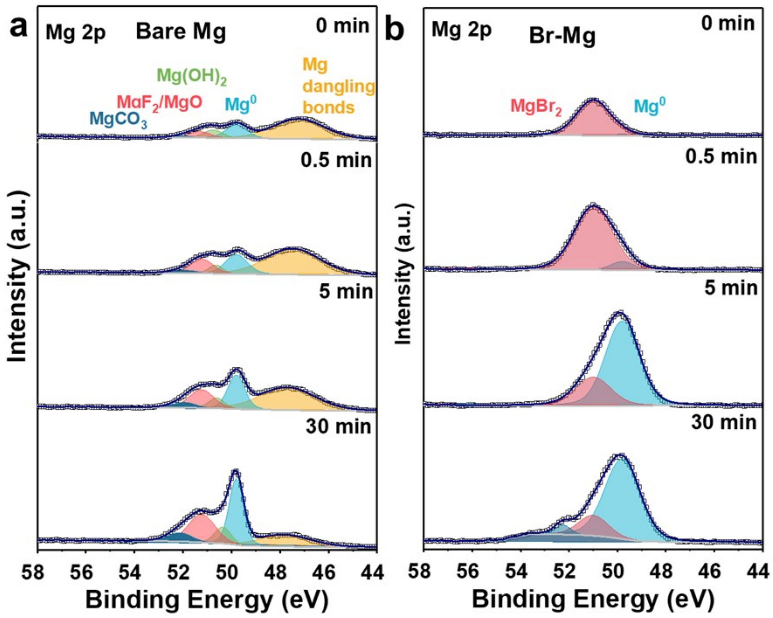

Figure S11. Depth profiling XPS Mg 2p spectra of anodes after cycling.

Table S1. XPS fitting details of Mg 2p peaks of bare Mg and Br-Mg anodes.

Electrode	Etching time (min)	Concentration of fitted components (%)					
		Mg^0	$Mg(OH)_2$	MgO	$MgBr_2$	$Mg(CO)_3$	Dangling bonds
Bare Mg	0	30.49	9.12	27.65	-	4.36	28.38
	0.5	29.28	11.56	30.18	-	3.13	25.84
	5	35.52	7.68	24.49	-	7.12	25.19
	30	45.95	7.74	21.98	-	6.36	17.96
Br-Mg	0	90.57	-	-	9.43	-	-
	0.5	69.71	-	-	30.29	-	-
	5	73.87	-	-	26.13	-	-
	30	76.40	-	-	23.60	-	-

Table S2. XPS fitting details of Br 3d peaks of Br-Mg anodes.

Electrode	Etching time (min)	Concentration of fitted components (%)	
		Organic-Br	$MgBr_2$
Br-Mg	0	84.67	15.33
	0.5	-	100
	5	-	100
	30	-	100

Table S3. Calculated parameters from EIS fitting curves before cycling.

Electrode	R_s (Ω)	R_{SEI} (Ω)	R_{ct} (Ω)
Bare Mg	46.55	-	840761
Br-Mg	5.56	25.86	334467

Table S4. Calculated parameters from EIS fitting curves measured at different temperatures.

Electrode	Temperature °C	R_s (Ω)	R_{SEI} (Ω)	R_{ct} (Ω)
Bare Mg	30	3.05	-	290412
	40	2.56	-	148633

	50	3.45	-	113052
	60	3.40	-	74298
Br-Mg	30	3.97	18.01	182947
	40	12.43	26.05	125081
	50	11.75	23.31	88043
	60	4.44	28.25	55679

Table S5. Calculated parameters from EIS fitting curves measured at different cycles.

Electrode	**Cycle number**	**R_s (Ω)**	**R_{SEI} (Ω)**	**R_{ct} (Ω)**
Bare Mg	10	6.55	3.29	287
	50	12.27	6.7	27614
	100	136.8	3.67	61070
	200	11.69	9.14	37426
Br-Mg	10	3.19	2.16	29.48
	50	33.46	2.82	20085
	100	3.01	3.71	88082
	200	4.52	2.96	57114

Table S6. Performance comparison of our symmetric cells with previous reports based on Mg electrode modification.

Electrode	**Electrolyte**	**Current density (mA/cm^2)**	**Areal capacity (mAh/cm^2)**	**Cycling life (h)**	**Overpotential (mV)**	**Reference**
c-PAN-Mg	$Mg(TFSI)_2$/PC	0.01	0.005	1000	500	[2]
MgF_2@Mg	APC	0.25	0.25	200	25	[3]
Bi-Mg	$Mg(TFSI)_2$/DME	1	0.5	4000	600	[4]
Mg-Si	$Mg(TFSI)_2$/DME	0.1	1	1400	300	[5]
MOF/Mg	$Mg(TFSI)_2$/DME	0.05	-	100	750	[6]
Mg-Bi@PTHF	$Mg(TFSI)_2$/DME	0.1	0.05	2000	200	[7]
Br-Mg	$Mg(TFSI)_2$/G2	1	0.5	150	500	[8]
Sb-Mg/$MgCl_2$@Mg	$Mg(OTf)_2$ + $MgCl_2$	1	1	1200	180	[9]
GPL@Mg	$Mg(TFSI)_2$/G2	0.5	0.5	200	340	[10]
LiI-Mg	$Mg(TFSI)_2$/DME	0.5	0.5	500	500	[11]
Sb-Mg	$Mg(TFSI)_2$/DME	0.2	0.2	800	250	[12]
Mg-Sn-Bi@Mg	APC	0.2	0.2	1000	53	[13]
In/$MgCl_2$@Mg	APC	1	0.5	1800	90	[14]
FRAB@Mg	$Mg(TFSI)_2$/DME	1	1	2200	600	[15]
PDG-Mg	$Mg(OTf)_2$ + $MgCl_2$/DME	1	1	900	200	[16]
MBI@Mg	$Mg(TFSI)_2$/DME	1	0.5	1750	230	[17]
In/MgI_2@Mg	$Mg[B(hfip)_4]_2$/DME	0.5	0.25	725	80	[18]
Al/OCI@Mg	$Mg[B(hfip)_4]_2$/DME	1	0.5	1200	180	[19]
Br-Mg	**$Mg[B(hfip)_4]_2$/DME**	**0.5 1 5**	**0.5 1 5**	**1610 1330 263**	**68 75 170**	**This work**

Table S7. Performance comparison of our symmetric cells with previous reports based on boron-centered electrolytes.

Electrode	**Electrolyte**	**Current density (mA/cm^2)**	**Areal capacity (mAh/cm^2)**	**Cycling life (h)**	**Overpotential (mV)**	**Reference**
Mg	MgFPB/G2	0.1	-	500	60	[20]
Mg	$Mg[B(hfip)_4]_2$+ PS +I_2/DME	0.1	0.05	700	102	[21]
Mg	$Mg[B(hfip)_4]_2$ + MgI_2/DME	0.5	0.25	500	93	[22]
Mg	$Mg[B(hfip)_4]_2$/DME-THF	0.1	0.1	2000	40	[23]

Mg	$Mg[B(hfip)_4]_2$ + $Bi(OTf)_3$ /DME	1	0.5	500	140	[24]
Mg	$Mg[B(hfip)_4]_2$/G2	1	0.5	47	80	[25]
Mg	$Mg[B(hfip)_4]_2$/DME	0.1	0.05	1200	90	[26]
Mg	BMCM/DME	0.1	0.05	500	68	[27]
Mg	TMPL-*n*$B(Otfe)_3$/THF	0.5	0.25	1000	128	[28]
In/MgI_2@ Mg	$Mg[B(hfip)_4]_2$/DME	0.5	0.25	725	80	[18]
Al/OCI@ Mg	$Mg[B(hfip)_4]_2$/DME	1	0.5	1200	180	[19]
Br-Mg	**$Mg[B(hfip)_4]_2$/DME**	**0.5 1 5**	**0.5 1 5**	**1610 1330 263**	**68 75 170**	**This work**

Table S8. Comparative table of asymmetric cell performance with previously reported boron-centered electrolytes.

Electrolyte	Current density (mA/cm^2)	Areal capacity (mAh/cm^2)	Cycles (number)	Coulombic efficiency (%)	Reference
TMPL-*n*$B(Otfe)_3$/THF	0.5	0.25	100	98.70	[28]
BMCM/DME	0.5	0.5	500	97	[27]
MCBB/THF	0.5	0.5	140	93	[29]
MBA-$B(Otfe)_3$/THF	0.5	-	200	98	[30]
$Mg[B(hfip)_4]_2$/DME	0.5	-	100	98	[31]
$Mg[B(hfip)_4]_2$/G3	0.5	0.25	100	98	[32]
$Mg[B(hfip)_4]_2$/DME-THF	0.5	0.25	500	99.40	[23]
$Mg[B(hfip)_4]_2$/DME	5	1	1000	99.04	[33]
$Mg[B(hfip)_4]_2$/DME	0.5	0.25	1000	96.90	[18]
$Mg[B(hfip)_4]_2$/DME	1	0.5	200	97.51	[19]
$Mg[B(hfip)_4]_2$/DME	**0.5**	**0.5**	**1630**	**99.50**	**This work**

Table S9. XPS fitting details of Mg 2p of bare Mg and Br-Mg anodes after 20 cycles in symmetric cells.

Electrode	Etching time (min)	Concentration of fitted components (%)					
		Mg^0	$Mg(OH)_2$	MgF_2/MgO	$MgBr_2$	$Mg(CO)_3$	Dangling bonds
Bare Mg	0	17.53	9.49	8.15	-	2.34	62.50
	0.5	18.22	5.16	13.64	-	3.02	59.96
	5	22.62	6.46	17.44	-	4.76	48.72
	30	34.39	9.74	27.12	-	7.59	21.16
Br-Mg	0	2.07	-	-	97.93	-	-
	0.5	7.48	-	-	92.52	-	-
	5	74.03	-	-	25.97	-	-
	30	78.83	-	-	16.99	4.18	-

Table S10. XPS fitting details of Br 3d of Br-Mg anodes after 20 cycles in symmetric cell.

Electrode	Etching time (min)	Concentration of fitted components (%)	
		Organic-Br	$MgBr_2$
Br-Mg	0	67.17	32.83
	0.5	-	100
	5	-	100
	30	-	100

References

1. D.-T. Nguyen, A. Y. S. Eng, M.-F. Ng, V. Kumar, Z. Sofer, A. D. Handoko, G. S. Subramanian and Z. W. Seh, *Cell Reports Physical Science*, 2020, **1**, 100265.
2. S. B. Son, T. Gao, S. P. Harvey, K. X. Steirer, A. Stokes, A. Norman, C. Wang, A. Cresce, K. Xu and C. Ban, *Nat Chem*, 2018, **10**, 532-539.
3. B. Li, R. Masse, C. Liu, Y. Hu, W. Li, G. Zhang and G. Cao, *Energy Storage Materials*, 2019, **22**, 96-104.
4. Y. Zhao, A. Du, S. Dong, F. Jiang, Z. Guo, X. Ge, X. Qu, X. Zhou and G. Cui, *ACS Energy Letters*, 2021, **6**, 2594-2601.
5. Y. Li, X. Zhou, J. Hu, Y. Zheng, M. Huang, K. Guo and C. Li, *Energy Storage Materials*, 2022, **46**, 1-9.
6. Y. Zhang, J. Li, W. Zhao, H. Dou, X. Zhao, Y. Liu, B. Zhang and X. Yang, *Adv Mater*, 2022, **34**, e2108114.
7. Y. Zhuang, D. Wu, F. Wang, Y. Xu, J. Zeng and J. Zhao, *ACS Appl Mater Interfaces*, 2022, **14**, 47605-47615.
8. A. R. Jeon, S. Jeon, G. Lim, J. Jang, W. J. No, S. H. Oh, J. Hong, S. H. Yu and M. Lee, *ACS Nano*, 2023, **17**, 8980-8991.
9. Y. Li, G. Yang, C. Zhang, W. Y. Lieu, C. Y. J. Lim, S. Sun, J. Wang, S. Jiang, Z. Xing, Z. Sofer, M. F. Ng, W. Liu and Z. W. Seh, *Advanced Functional Materials*, 2023, **33**, 2210639.
10. S. Shin, J. H. Kwak, S. H. Oh, H. S. Kim, S. H. Yu and H. D. Lim, *ACS Appl Mater Interfaces*, 2023, **15**, 28684-28691.
11. C. Wang, H. Huang, X. Wu, M. Yousaf, M. Yan and Y. Jiang, *ACS Appl Mater Interfaces*, 2023, **15**, 51126-51134.
12. B. Yang, L. Xia, R. Li, G. Huang, S. Tan, Z. Wang, B. Qu, J. Wang and F. Pan, *Journal of Materials Science & Technology*, 2023, **157**, 154-162.
13. X. Chai, H. Xie, T.-T. Zhang, Y. Xin, F. Zhang, B. He, H. Xie, L. Yu and H. Tian, *Energy Storage Materials*, 2024, **70**, 103460.
14. Y. Chen, X. Shen, J. Wang, Y. Zhang, Y. Hao, L. Tong, G. Huang, Q. Li, X. Zhou, B. Qu and F. Pan, *ACS Energy Letters*, 2024, **9**, 5616-5626.
15. G. Li, K. Chen, M. Lei, T. Wang, M. Hu and C. Li, *Advanced Energy Materials*, 2024, **14**, 2401507.
16. Y. Li, X. Feng, G. Yang, W. Y. Lieu, L. Fu, C. Zhang, Z. Xing, M. F. Ng, Q. Zhang, W. Liu, J. Lu and Z. W. Seh, *Nat Commun*, 2024, **15**, 9364.
17. D. Zhang, Y. Sun, X. Liu, Y. Zhang, R. Wang, Y. Zhao, M. Pan, Y. Wang, S. Chen, M. Zhou, Y. Chen, J. Yang, J. Wang and Y. NuLi, *ACS Energy Letters*, 2024, **9**, 2685-2695.
18. S. Cao, X. Qi and X. Zhao, *Energy & Fuels*, 2025, **39**, 15498-15504.
19. Y. Chen, Y. Zhang, Z. Tang, Z. Zhang, L. Tong, X. Gan, X. Shen, G. Huang, Q. Li, B. Qu, F. Pan and J. Wang, *Chemical Engineering Journal*, 2025, **521**, 166781.
20. J. Luo, Y. Bi, L. Zhang, X. Zhang and T. L. Liu, *Angew Chem Int Ed Engl*, 2019, **58**, 6967-6971.
21. V. B. Parambath, Z. Zhao-Karger, T. Diemant, M. Jäckle, Z. Li, T. Scherer, A. Gross, R. J. Behm and M. Fichtner, *Journal of Materials Chemistry A*, 2020, **8**, 22998-23010.
22. X. Song, J. Sun, W. Ren, L. Wang, B. Yang, H. Ning, P. Zhang, Z. Caixiang, Z. Tie, X. Zhang, Y. NuLi and Z. Jin, *Angew Chem Int Ed Engl*, 2025, **64**, e202417450.
23. C. Chen, J. Chen, S. Tan, Z. Gao, X. Huang, Z. He, J. Huang, R. Deng, F. Xiong, G. Huang, J. Wang, L. Li and F. Pan, *Advanced Functional Materials*, 2025, **n/a**, 2505843.
24. Z. Meng, Z. Li, L. Wang, T. Diemant, D. Bosubabu, Y. Tang, R. Berthelot, Z. Zhao-Karger and M. Fichtner, *ACS Appl Mater Interfaces*, 2021, **13**, 37044-37051.

25. J. Drews, P. Jankowski, J. Hacker, Z. Li, T. Danner, J. M. Garcia Lastra, T. Vegge, N. Wagner, K. A. Friedrich, Z. Zhao-Karger, M. Fichtner and A. Latz, *ChemSusChem*, 2021, **14**, 4820-4835.
26. Z. Zhao-Karger, R. Liu, W. Dai, Z. Li, T. Diemant, B. Vinayan, C. Bonatto Minella, X. Yu, A. Manthiram and R. J. r. Behm, *ACS energy letters*, 2018, **3**, 2005-2013.
27. X. Huang, J. Wen, J. Lei, G. Huang, F. Pan and L. Li, *ACS Applied Materials & Interfaces*, 2022, **14**, 8906-8915.
28. Y. Wang, Y. Sun, D. Zhang, M. Pan, Y. Chen, S. Chen, S. Zhang, Y. Zhao, J. Wang and Y. NuLi, *Energy Storage Materials*, 2024, **65**, 103152.
29. M. Cheng, W. Ren, D. Zhang, S. Zhang, Y. Yang, X. Lv, J. Yang, J. Wang and Y. NuLi, *Energy Storage Materials*, 2022, **51**, 764-776.
30. W. Ren, D. Wu, Y. NuLi, D. Zhang, Y. Yang, Y. Wang, J. Yang and J. Wang, *ACS Energy Letters*, 2021, **6**, 3212-3220.
31. Z. Zhao-Karger, M. E. G. Bardaji, O. Fuhr and M. Fichtner, *Journal of Materials Chemistry A*, 2017, **5**, 10815-10820.
32. T. Mandai, *ACS Appl Mater Interfaces*, 2020, **12**, 39135-39144.
33. S. Li, J. Zhang, S. Zhang, Q. Liu, H. Cheng, L. Fan, W. Zhang, X. Wang, Q. Wu and Y. Lu, *Nature Energy*, 2024, **9**, 285-297.